Cluster state preparation using gates operating at arbitrary success probabilities

K. Kieling, D. Gross, and J. Eisert
Blackett Laboratory, Imperial College London, Prince Consort Road, London SW7 2BW, UK and
Institute for Mathematical Sciences, Imperial College London, Prince's Gate, London SW7 2PG, UK
(Dated: March 8, 2007)

Several physical architectures allow for the sequential preparation of cluster states for measurement-based quantum computing using probabilistic quantum gates. In such an approach, the order in which partial resources are combined to form the final cluster state turns out to be crucially important. We determine the influence of this classical decision process on the expected size of the final cluster. Extending earlier work, we consider different quantum gates operating at various probabilites of success. For finite resources, we employ a computer algebra system to obtain the provably optimal classical control strategy and derive symbolic results for the expected final size of the cluster. Surprisingly, two substantially different regimes can be identified: When the success probability of the elementary gates is high, the influence of the classical control strategy is found to vanish. In that case, other figures of merit become more relevant. For small probabilities of success, the choice of an appropriate strategy is crucial.

PACS numbers: 03.67.Lx, 03.67.Mn, 03.67.Pp

I. INTRODUCTION

Measurement-based quantum computing has a number of appealing features not present in the standard gate model. From an experimental perspective, it may well be a significant advantage to abandon the need for exact unitary control between any two constituents, and separate the process of entanglement generation from that of entanglement consumption. In such measurement-based computing, an entangled state is generated, followed by a sequence of local measurements on single constituents. In the original one-way computer [1], this universal resource is the cluster state [2]. In the following, we will indeed concentrate on cluster state preparation; see, however, Ref. [3] for a method of constructing a number of novel models for measurement-based computing that make use of resource states different from the cluster state.

Generally speaking, there are two ways of preparing cluster states: On the one hand, this can be done by means of translationally invariant local interactions, not requiring individual local control. This most prominently applies to preparations using cold collisions of atoms in optical lattices by applying spin-dependent shifts [4, 5]. The other way is to build up cluster states from *elementary building blocks*, such as entangled pairs, a framework we will concentrate on in this work. This is the setting that plays the key role when applied to a number of physical architectures: Specifically, it is the preferable or typically only applicable method in preparations using linear optical systems [6, 7, 8, 9, 10], optical systems with weak non-linearities [11], trapped atoms [12], and matter qubits in optical cavities [13, 14, 15, 16, 17]. Here, the quantum gates that are applied are typically inherently probabilistic, necessarily leading to a significant overhead in required resources. For linear optical settings in particular, the probabilistic character is unavoidable [18, 19].

There is a new element in this idea, that was not present before: *Choice*. Indeed, when building up resource states from smaller blocks, several kinds of intermediate structures will appear, and it turns out to be crucial to make a meaningful choice of which parts to attempt to link at what stage. This is no marginal effect, but can give rise to differences in orders of magnitude in, say, consumption of EPR pairs, even for moderately-sized cluster states [20], so maximally entangled photon pairs in the optical context. Fortunately, for building up cluster chains using gates with elementary success probability of the gate of $p_{\rm s} > 0$, an overhead is sufficient that is linear in the size of the final chain [10, 20]. For the special case $p_{\rm s} = 1/2$ (e.g., linear optics) five EPR pairs per edge is an upper bound for the optimal strategy, a bound that can not be improved any more with sequentially acting gates operating at the success probability dictated by linear optics. Further, for any $p_{\rm s} > 0$ the overhead required to produce a 2D cluster out of chains is also only linear in the size of the state to produce. As all these processes are probabilistic, the quoted results actually state that a constant overhead per site is sufficient for any $p_{\rm s} > 0$ to produce a state of size $n \times n$ (or n in the 1D case) almost certainly as n becomes large [10].

For other elementary probabilities $p_{\rm s} > 0$, what is the method of choice of dealing with the intrinsic randomness? This is the question that we address in this work, complementing recent investigations [10, 20] and numerical work on this topic [21] (see also [22]). In contrast to Refs. [10, 20], where also rigorous asymptotic bounds have been presented, we here solely investigate the optimal and worst strategies for finite N using a computer-assisted proof, for arbitrary $p_{\rm s}$ and different gates. We discuss also the algorithm which is capable of finding the provably optimal classical control strategy and delivers symbolic results for the expected final size of the cluster. Further, some detailed numbers on the resource consumption in the preparation of 2D cluster states are given.

II. TECHNIQUES

In the first part of this work we aim at building up linear cluster chains from a reservoir of N maximally entangled pairs. Our interest lies in finding the optimal classical control strategy – hence it will be fruitful to abstract from the underlying quantum system. Indeed, at a given point in the process of

Gate	d_f	d_s	Physical realization
CZ	2	1	Distant atoms [12, 14]
KLM CZ	1	1	Linear optics with $p_\mathrm{s} = 1/16$ [6] or $p_\mathrm{s} = 1/4$ [23]; weak non-linearities with $p_\mathrm{s} = 3/4$ [11]; linear optics with $p_\mathrm{s} = p_\mathrm{NDM}/9$ [24, 25]; $p_\mathrm{s} = 1/8$ [9]
DPC	2	0	Trapped atoms and frequency qubits [13], $p_\mathrm{s} < 1/4$
Fusion	1	0	Linear optics parity check [7], optimal $p_\mathrm{s} = 1/2$ [10]

TABLE I: The four quantum gates described in the text. $(d_\mathrm{s}, d_\mathrm{f})$ denote the number of edges deleted per chain on failure and the number of chains gained on success, respectively. p_NDM is the probability of success of a photon number non-demolition measurement that has to follow the respective gate.

building up the cluster, we have a collection of cluster chains of various lengths at our disposal. The "state" of our system can hence solely be described by the respective lengths of the chains. This information will be represented by a *configuration* vector $c = (c_1, c_2, \ldots, c_\mathrm{max})$, where c_i is the number of chains of length i, as counted by the number of edges. An EPR pair, a maximally entangled qubit pair, has hence length 1.

For the task of joining intermediate cluster states together to form longer chains, we employ entangling gates like the Type-I fusion gate [7]. We restrict ourselves to two qubit gates that act symmetrically and with the same action for chains of all lengths – most suggested quantum gates do have this property. The effective actions on two chains of lengths l_1 and l_2 in the number of edges can then be described by the outcomes on *success* and *failure*,

$$\{l_1, l_2\} \mapsto \{l_1 + l_2 + d_\mathrm{s}\}, \quad (1)$$

$$\{l_1, l_2\} \mapsto \{l_1 - d_\mathrm{f}, l_2 - d_\mathrm{f}\}, \quad (2)$$

respectively, and are cast into the tuple $(d_\mathrm{s}, d_\mathrm{f})$. This family embodies four gates: On the one hand it contains two with an undefined failure outcome. To obtain a proper cluster state, additional Z-measurement on the neighbors has to cut off the end qubits, thus $d_\mathrm{f} = 2$. Additionally, there are those gates with a "built-in" Z-measurement on failure, $d_\mathrm{f} = 1$. On the other hand, there are two "parity check" gates (no new edges are created, $d_\mathrm{s} = 0$) and controlled-Z (entanglement is created, $d_\mathrm{s} = 1$). See table I for more details.

We can now describe our model for the generation of cluster states. Starting point is a configuration consisting of N EPR pairs. In each step of the process, we choose two chains out of the repository and try to fuse them. The choice which specific two chains to take is determined by the classical *strategy*. A strategy is hence a complete prescription which chains to fuse for all possible configurations that may occur. The process continues until either i) there is only a single chain left or ii) the strategy decides to keep only the longest chain in the current configuration and to disregard the rest. Note that for the case $p_\mathrm{s} = 1/2$ – of central importance in linear optical architectures – one never benefits from halting before all smaller

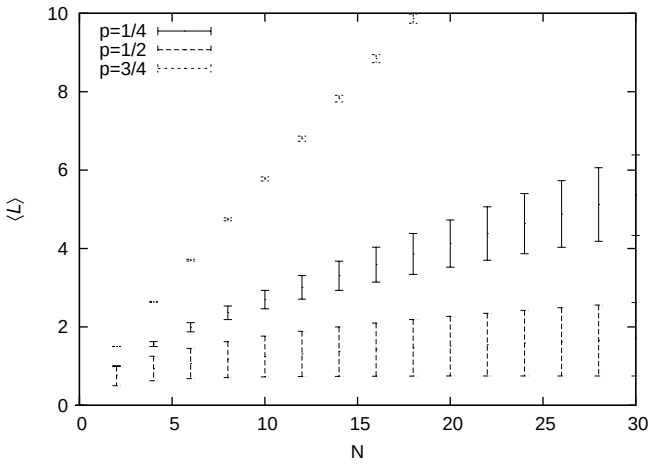

FIG. 1: The graphs show the influence of the classical strategy on the expected length of the final cluster for Type-I fusion gates operating at $p_\mathrm{s} = 1/4, 1/2$ and $3/4$ respectively. For each probability, the range enclosed by the error bars indicates the spread between the best possible and worst possible strategy.

chains have been consumed [10]. The performance of the strategy can then be measured by the expected length of the longest chain in the final configuration: Since this is a probabilistic process, the outcome will in general be an expectation value $\langle L \rangle$ of the final length over all possible final configurations. Note that there are two different means involved here: On the one hand, there is the distribution of cluster states of different lengths in a given configuration. On the other hand, since cluster state preparation is a probabilistic process, there is the distributions of configurations in the first place. It is the role of these two different means that renders the discussion of the influence of the classical strategy involved.

We will obviously be interested in the performance of the optimal strategy, $Q = \langle L \rangle_\mathrm{opt}$, which we will also refer to as *quality* of the strategy. We will also pay quite a significant attention to the worst strategy, however, to assess what influ-

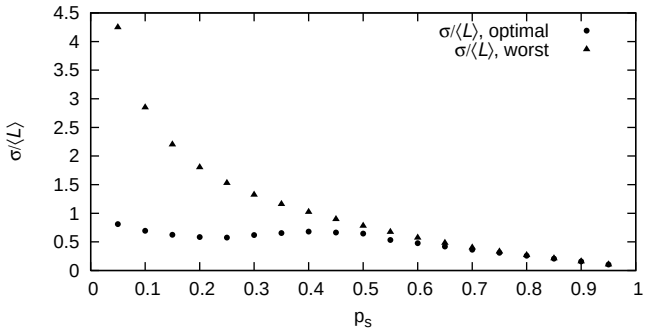

FIG. 2: Relative standard deviation $\sigma/\langle L \rangle$ of the distribution of final chains for the optimal and worst strategy respectively. It turns out that for high success probabilities, the statistical fluctuations for a single fixed strategy are more pronounced than the the difference between even the best and the worst strategy.

ence the decision process can possibly have. More concretely, we will ask what is the shortest expected length one can obtain out of N initial EPR pairs, if one continues to try to fuse all intermediate resources together until only a single chain is left.

III. ARBITRARY GATE PROBABILITIES

Depending on the physical context, p_s can vary over quite a range of different values. In the *linear optical context*, $p_s = 1/2$ plays a prominent role as the optimal success probability of the parity check gate [10]. When taking inefficient detectors into account, needless to say, this success probability will rapidly decrease below the theoretical value of $p_s = 1/2$.

In Ref. [13], probabilistic quantum gates on remote *trapped atom qubits* have been considered, exploiting interference of optical frequency qubits. Here, the success probability p_s is relatively small, smaller than $1/4$ even for perfect photon detectors. However, the respective measurement gate is constructed in a way to be very robust with respect to noise. We will see that for these kind of gates operating at a relatively low probability of success, the choice of strategy is in fact crucial.

However, gates constructed using *weak non-linearities* in optical systems as considered in Refs. [11] can result in $p_s = 1 - 2^{-1-n}$ where n is the number of ancillas used [11]. In this context, we will see that the worst strategy performs essentially identical to the optimal strategy, hence confirming that in the regime of high success probability, strategic choice hardly matters.

In contrast to other approaches, we give exact values for the optimal and the worst strategy. Furthermore, we will stick to our previous notion of strategies acting on a fixed reservoir of resource states. However, using Theorem 16 from Ref. [10], these results also deliver the solution to the inverse question, of the average resource consumption for construction of a chain of given length (see [21] for numerical results on the inverse question, namely the generation of fixed length chains using an infinite supply of entangled pairs).

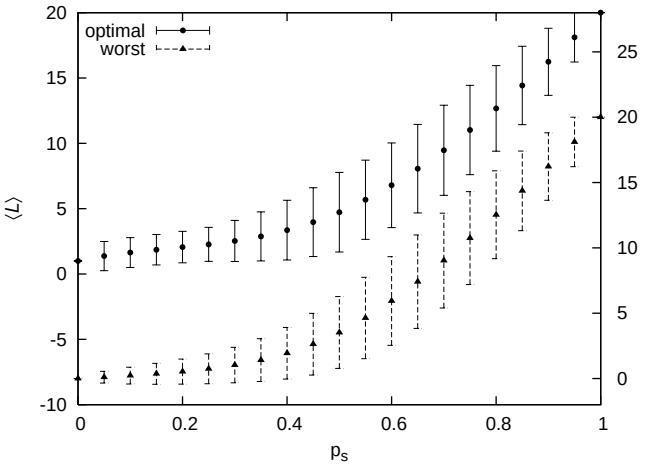

FIG. 3: Expected final length of the optimal and the worst strategy, starting from $N = 20$ EPR pairs. Error bars give the standard deviation of the final length distributions. For better visibility, "worst" is shifted downwards, its y-axis is the right one.

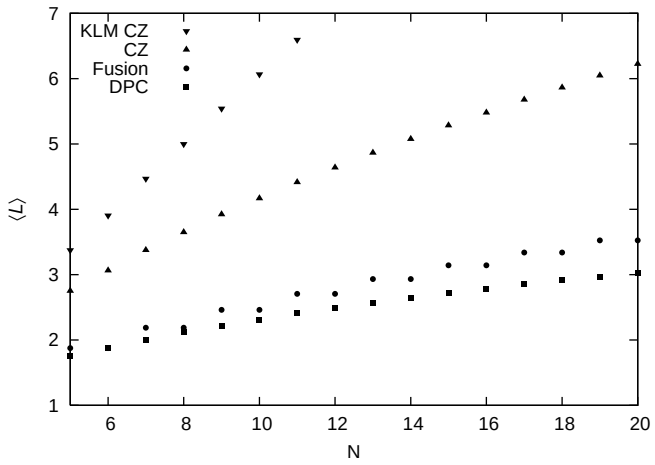

FIG. 4: The optimal expected length $\langle L \rangle$ of the final cluster for the gates listed in Table I.

Figure 1 shows how the optimal and the worst strategy perform when using the Type-I fusion gate at different probabilities. Examples from three different *regimes* are shown, the distinctness of which is quite remarkable:

- For small gate probabilities the choice of strategy is crucial. Applying gates in a particularly unfortunate fashion might actually result in no net increase of the length of the longest chain at all. However, employing the optimal strategy the length of the longest chain turns out to be an increasing function of the number of EPR pairs, rather than a constant one.

- In some intermediate regime (like $p_s = 1/2$ for Type-I fusion gate) both the optimal as well as the worst strategy result in a length increase of the longest chain. But still, the choice of strategy distinguishes whether an efficient growth, i.e., a linear growth $O(n)$ will be obtained, in constrast to merely a growth of $O(\sqrt{n})$.

- For p_s being large, the difference in the performance of strategies becomes negligible for practical purposes. The order in which the fusion attempts are carried out hence hardly matters. This comes in handy as one does not have to concentrate on the optimal strategy in experimental realizations any more. Even though the optimal strategy also realizes the least storage time in this setting, there is also almost no difference in the amount of storage time required by the different strategies. Then, of course other meaningful figures of merit enter center stage, like the amount of feed-forward or rerouting needed. Strategies like STATIC [10] that only fuse nearest neighbors in the repository of chains will then be favorable as they realize the least amount of feed-forward in this setting simultaneously.

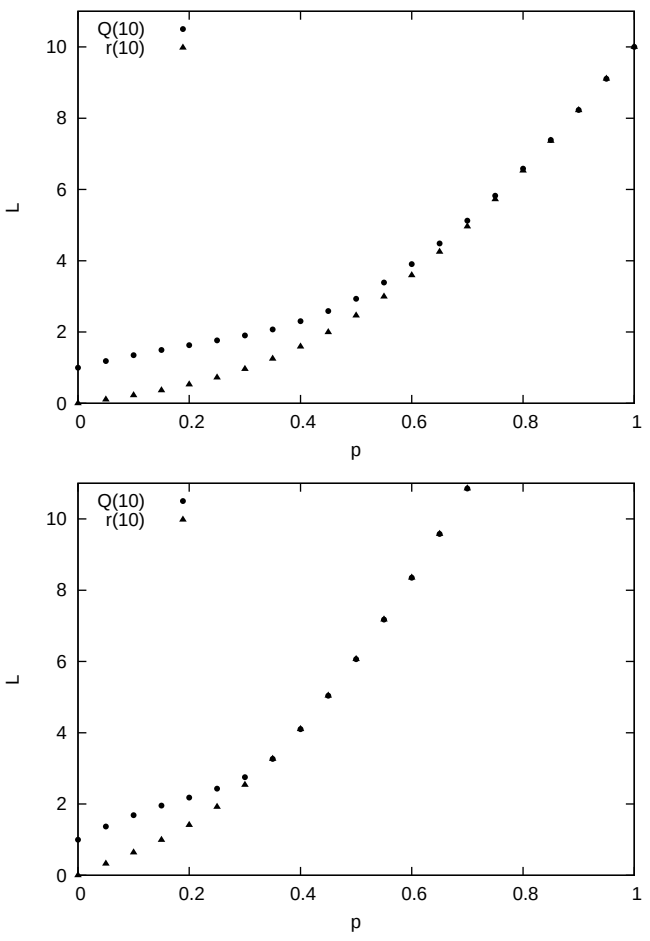

FIG. 5: Performance of the optimal and worst strategy for $N = 10$ for Type-I fusion (upper graph) and the KLM controlled-Z gate (lower graph). Both gates have the same number of lost edges on failure.

Note that, however, no feed-forward in this setting means no shuffling around of chains rather than single qubits. A huge amount of rerouting on the level of qubits is still needed. See Ref. [27] for a possible solution to this problem, making use of percolation ideas.

Figures 2 and 3 show the dependence of the standard deviation σ of the final length distributions on the gate probability. As the gate probability increases not only the upper and lower bound to strategy performances converge, but also their relative variances converge and vanish. Interestingly enough, the relative difference between the two strategies gets even smaller than their relative standard deviations.

IV. ADDITIONAL GATES

The action of all gates used here can be described by a pair of two parameters $(d_\mathrm{f}, d_\mathrm{s})$ (similar to the treatment in [21]): The number of edges that are deleted from the participating chains in case of failure d_f and the number of edges d_s that are added when successful. The Type-I fusion gate deletes the participating qubits in case of failure. The length of the resulting chain on success is the sum of the lengths of the original chains. Therefore, this gate can be described by the parameters $(1, 0)$. Besides having investigated its performance at different success probabilities, we further compared it to other possible entangling gates. The general controlled-Z gate creates an edge between the qubits it is acting on. However, on failure the outcome is not known [21] and the two qubits have to be cut by applying Z-measurements to the neighboring sites. Thus, this gate effectively deletes 2 edges from both chains on failure, and it is represented by $(2, 1)$. The KLM CZ gate [6] has, in contrast, a defined error outcome which is effectively the action of a Z-measurement on the two qubits. Therefore, this gate simply cuts the two qubits from their chains on failure, and consequently is characterized by $(1, 1)$. For the sake of completeness we also introduce a gate which does not add any new edges (like the fusion gate), but deletes two edges from each chain on failure (like the CZ gate), thus resulting in $(2, 0)$. This gate might be a parity check gate, like the fusion gate, but with an undefined failure outcome, thus denoted by DPC (destructive parity check). Actually, the individually trapped atoms can be used to implement this type of gate [13].

Further gates would be for example the Type-II fusion [7], or the one created by weak non-linearities using the qubus technique [11]. However, the first one is hard to compare with the gates presented here as it requires GHZ resources, rather than EPR pairs. The latter one is actually already included in our analysis, as it corresponds to a gate with parameters $(1, 1)$, operating with a gate-probability $p_\mathrm{s} = 3/4$.

The performance $\langle L \rangle_\mathrm{opt}$ of the optimal strategy using all four gates is shown in figure 4. The difference between the gates in the number of edges consumed on success and on failure is clearly reflected by the optimal average final length that is achieved. As noted earlier, we do observe an interesting crucial dependence of the performance of the best and worst strategy while varying p_s: $1/2$ marks some *intermediate regime* for the Type-I fusion gate, above which the choice of strategy does not carry weight anymore. This behavior is indicated by the diminishing gap in the first part of figure 5. The second part shows this plot using the KLM CZ gate. Interestingly, in this case the worst and optimal strategy are already indistinguishable at gate probabilities far below $1/2$. Not only the probability, but also which type of gate is used influences how important the classical choice of strategies will be.

V. ALGORITHM

Can one use a computer-assisted proof to identify the optimal strategy for a given configuration? Naively, one would expect this not to be the case, as the number of configurations with n entangled bonds is exponential in n [10] and the number of strategies is, in turn, exponential in the number of configurations. So a brute-force search for the optimal strategy is clearly unfeasable. Fortunately, the problem can be addressed using a smarter, recursive algorithm, as a variant of a backtracking algorithm.

NAME:	Optimize
INPUT:	Integer n
OUTPUT:	For all configurations C with up to n vertices, the global variable $Q(C)$ is set to the quaity of C.

```
1   SUB Optimize(n)
2     for i := 1 to n
3       C := AllConfs(n)
4       foreach c ∈ C
5         OptimizeConf(c)
6       end foreach
7   end for
```

NAME:	OptimizeConf
INPUT:	Configuration c
ASSUMPTION:	For all configurations c' with fewer particles than c, the global variable $Q(c')$ is set to the quality of c'.
OUTPUT:	Sets global variable $Q(c)$ to quality of c.

```
1   SUB OptimizeConf(c)
2     l := length(c)
3     for i ≤ l
4       for j < i
5         q[i,j] := p Q(fuse(c,i,j)) + (1-p)Q(fail(c,i,j))
6       end for
7     end for
8     Q(c) := max_{i,j} q[i,j]
```

FIG. 6: The recursive algorithm which computes the optimal expected length one can obtain from a given configuration. It relies on three simple sub-routines: $\mathrm{AllConfs}(n)$, which returns a table of all possible configurations with up to n particles; $\mathrm{fuse}(c,i,j)$, returning the configuration resulting from c after a successful fusion of the i-th and j-th chain and finally $\mathrm{fail}(c,i,j)$ which acts likewise, but assumes the fusion to fail.

To understand how, note that as a result of an attempted fusion, the number of entangled particles decreases by one in case of success and by at least two in case of failure. Now consider a given configuration c with n vertices (not edges) and assume that we know the quality Q for all configurations of strictly fewer than n constituents. If the number of chains in c equals l, then there are roughly l^2 possible choices a strategy can make. If the strategy decides on fusing chains i and j, then the expected final length is going to be

$$p\,Q(\mathrm{fuse}(c,i,j)) + (1-p)Q(\mathrm{fail}(c,i,j)). \qquad (3)$$

The preceeding value can be computed explicitly, because by assumption Q is known for both $\mathrm{fuse}(c,i,j)$ and $\mathrm{fail}(c,i,j)$. Hence, using $O(l^2)$ tests, one can identify the optimal pair (i,j).

A computer implementation builds up a lookup table, i.e., a list containing the quality Q of every configuration up to a given number of particles n. The process starts with the the trivial configuration $n = 2$, for which the quality is known and works its way up to higher n as described before.

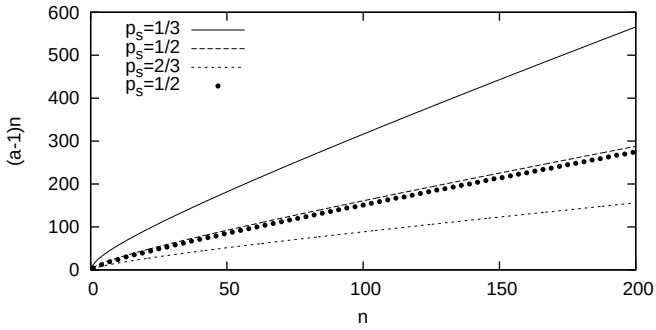

FIG. 7: Overhead $(a-1)n$ in the weaving provess with elementary probability $p_\mathrm{s} = 1/3, 1/2, 2/3$ to succeed for cluster size n with a probability of at least $P_\mathrm{s} = 19/20$. In addition to the upper bounds, exact values for $p_\mathrm{s} = 1/2$ are given.

Figure 6 presents an explicit pseudo-code implementation. By adjusting the parameter p and the subroutines $\mathrm{fail}()$ and $\mathrm{fuse}()$, the program is easily modified to general gates. Also note that finding the *worst* possible strategy can be achieved similarily.

The usefulness of practical implementations will be limited by memory consumption, as the lookup table grows linearly in the number of configurations, which is exponential in n. We utilized the computer algebra system *Mathematica* to assess the quality of configurations consisting of several dozen particles. A desktop computer completes the calculations in a few hours.

VI. PREPARATION OF 2D STRUCTURES: "WEAVING"

We now turn to the preparation of two-dimensional structures, universal for quantum computing. 2D cluster states can be generated starting from linear chains. Here, the probabilistic character of the employed quantum gates is again crucial: One has to make sure that the preparation becomes almost certain for large 2D cluster states. Fortunately, it turns out that this aim can always be achieved: As has been shown in Ref. [10] (compare also Refs. [22] for a strong indication suggesting a polynomial bound), starting from linear cluster chains, 2D cluster states of arbitrary size $n \times n$ can be built almost certainly for large n, with an overhead per site that only depends on the gate probability. Hence, the overall probability of success satisfies

$$P_\mathrm{s}(n) \to 1, \qquad (4)$$

when using $O(n^2)$ EPR pairs for a state of size $n \times n$. Moreover, this is true for any $p_\mathrm{s} > 0$. This is obviously the optimal scaling that can be achieved for 2D cluster states [10].

The gates necessarily act on qubits vertices located along the chain, and not only on vertices at the end of the chain. Hence, the employed quantum gates must provide suitable error outcomes in order not to tear the chains apart. Then, the

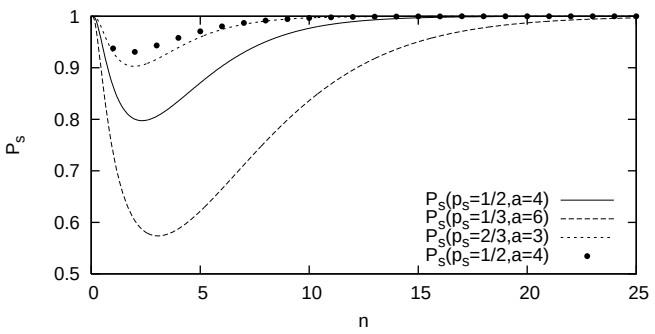

FIG. 8: The weaving success probability $P_{\rm s}(n)$ for fixed gate probability $p_{\rm s} = 1/3, 1/2, 2/3$ and overhead $a = 2/p_{\rm s}$. For $p_{\rm s} = 1/2$ exact values are given for comparison with the lower bound.

weaving procedure as proposed in Ref. [20] can be used to construct a cluster using gates succeeding with any $p_{\rm s} > 0$ almost certainly with a constant overhead per site. To find the actual prefactor of the leading quadratic term, we recall the processes that consume edges when constructing a site:

- The cluster construction itself – there are n^2 sites and $2n(n-1)$ edges.
- A σ_z measurement is applied to a qubit on one of the chains, destroying 2 edges.
- Failures of the fusion gate result in alternating deletions of two edges from the two chains involved.

Fixing an overall success probability results in a number of overhead edges that determines the number of possible failures. Up to a constant error per chain – thus only linear in n – the number of failures equals the number of edges consumed. The number of edges per chain depends linear on the side length of the cluster to be produced, the coefficient being a (see figure 7).

The lower bound for the overall success probability [10]

$$P_{\rm s}(n) \geq \left(1 - \exp\left(-\frac{2(anp_{\rm s} - n + 1)^2}{an}\right)\right)^n \qquad (5)$$

is displayed in figure 8. Chosing $a > 1/p_{\rm s}$ will result in $P_{\rm s}(n) \to 1$ as $n \to \infty$. By fixing n and $p_{\rm s}$ we can extract from (5) a for a given $P_{\rm s}$, so also the number of overhead edges that are required to achieve at least this overall success probability,

$$a = 1/p_{\rm s} + \varepsilon + o(1) \qquad (6)$$

with $\varepsilon > 0$. Figure 9 shows the dependence of the required resources on the gate probability $p_{\rm s}$. Summing up all these contributions we arrive at a resource consumption when building 2D clusters from existing chains of at least

$$4 + 2(1/p_{\rm s} - 1) \qquad (7)$$

per site, for example 9 edges at $p_{\rm s} = 1/2$.

This prefactor – so far the best known one – can possibly be improved still. For example, one may aim at not preparing a 2D cluster state, but a state that is equivalent to such a state, up to local unitary rotations. Specifically, one could aim at preparing a graph state that is equivalent to a cluster up to local Clifford operations. To investigate the orbit under such local Clifford operations is reflected on the level of graphs by local complementations [29, 30]. Ref. [31] already exploits such local complementations when efficiently preparing 2D structures. It would be interesting to see whether a systematic explorations of these tools give rise to a significant improvement of the above prefactor in the optimal quadratic scaling.

VII. SUMMARY

We have applied the tools introduced in Refs. [10, 20] to a number of different quantum gates to prepare cluster states for quantum computing from elementary blocks. Depending on the underlying physical architecture, the gates operate at different success probabilities. A qualitatively different behavior of the difference between the optimal and the worst outcomes has been observed when varying $p_{\rm s}$. The specific probability at which this transition occurs depends on the parameters of the gate used, i.e., how many edges are consumed on success and failure. At low probabilities the choice of strategy is highly significant, and any scheme for building up cluster states has to be based on a good choice of a strategy. For gates at high $p_{\rm s}$, the potential difference is negligible. Hence, in this regime, other figures of merit, minimizing imperfections and error proparation [26] in an actual experimental context, become the key quantities. This work provides a guideline to what extent the choice of the classical preparation strategy is crucial. Similar ideas could also be applied when building up structures that may be used for fault-tolerant or error resilient schemes [32, 33]. Needless to say, we have concentrated on the preparation of cluster states for measurement-based quantum computing. It would be interesting to see how the new freedom of quantum computing using universal resources different from cluster states as in Ref. [3] affects the strategies of

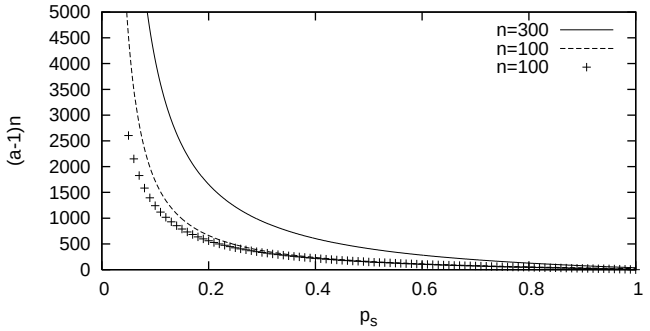

FIG. 9: Overhead $(a-1)n$ that is needed for the weaving process to succeed for a fixed cluster size $n = 100, 300$ with a probability of at least $P_{\rm s}(n) = 19/20$. For comparison with the upper bounds, exact values are given for $n = 100$ as well.

preparation.

Acknowledgements

We thank W.J. Munro for discussions. This work has been supported by the DFG, the EU (QAP), the EPSRC, QIP IRC, Microsoft Research through the European PhD Scholarship Programme, and the EURYI award scheme.

[1] H.J.- Briegel and R. Raussendorf, Phys. Rev. Lett. **86**, 5188 (2001).
[2] D.E. Browne and H.-J. Briegel, quant-ph/0603226; M. Hein, W. Dür, J. Eisert, R. Raussendorf, M. Van den Nest, and H.-J. Briegel, quant-ph/0602096.
[3] D. Gross and J. Eisert, quant-ph/0609149.
[4] D. Jaksch, H.-J. Briegel, J.I. Cirac, C.W. Gardiner, and P. Zoller, Phys. Rev. Lett. **82**, 1975 (1999).
[5] O. Mandel, M. Greiner, A. Widera, T. Rom, T.W. Hänsch, and I. Bloch, Nature **425**, 937 (2003).
[6] E. Knill, R. Laflamme, and G.J. Milburn, Nature **409**, 46 (2001).
[7] D.E. Browne and T. Rudolph, Phys. Rev. Lett. **95**, 010501 (2005).
[8] P. Walther, K.J. Resch, T. Rudolph, E. Schenck, H. Weinfurter, V. Vedral, M. Aspelmeyer, and A. Zeilinger, Nature **434**, 169 (2005).
[9] X.-H. Bao, T.-Y. Chen, Q. Zhang, J. Yang, H. Zhang, T. Yang, and J.-W. Pan, quant-ph/0610182.
[10] D. Gross, K. Kieling, and J. Eisert, Phys. Rev. A **74**, 042343 (2006).
[11] S.G.R. Louis, K. Nemoto, W.J. Munro, and T.P. Spiller, quant-ph/0607060.
[12] C. Cabrillo, J.I. Cirac, P. Garchia-Ferndandez, and P. Zoller, Phys. Rev. A **59**, 1025 (1999).
[13] L.-M. Duan, M.J. Madsen, D.L. Moehring, P. Maunz, R.N. Kohn Jr., and C. Monroe, quant-ph/0603285.
[14] L.M. Duan and H.J. Kimble, Phys. Rev. Lett. **90**, 253601 (2003).
[15] D.E. Browne, M.B. Plenio, and S. Huelga, Phys. Rev. Lett. **91**, 067901 (2003).
[16] S.D. Barrett and P. Kok, Phys. Rev. A **71**, 060310(R) (2005).
[17] Y.L. Lim, S.D. Barrett, A. Beige, P. Kok, and L.C. Kwek, Phys. Rev. A **73**, 012304 (2006).
[18] S. Scheel and N. Lütkenhaus, New J. Phys. **6**, 51 (2004).
[19] J. Eisert, Phys. Rev. Lett. **95**, 040502 (2005).
[20] K. Kieling, D. Gross, and J. Eisert, J. Opt. Soc. Am. B **24**, 184 (2007).
[21] P.P. Rohde and S.D. Barrett, quant-ph/0701068.
[22] L.-M. Duan and R. Raussendorf, Phys. Rev. Lett. **95**, 080503 (2005).
[23] T.B. Pittman, B.C. Jacobs, and J.D. Franson, Phys. Rev. A **64**, 062311 (2001).
[24] T.C Ralph, N.K. Langford, T.B. Bell, and A.G. White, Phys. Rev. A **65**, 062324 (2002).
[25] H.F. Hofmann and S. Takeuchi, Phys. Rev. A **66**, 024308 (2002).
[26] P.P. Rohde, T.C. Ralph, and W.J. Munro, quant-ph/0701090.
[27] K. Kieling, T. Rudolph, and J. Eisert, quant-ph/0611140.
[28] Q. Chen, J. Cheng, K.-L. Wang, and J. Du, Phys. Rev. A **73**, 012303 (2006).
[29] M. Hein, J. Eisert, and H.J. Briegel, Phys. Rev. A **69**, 062311 (2004).
[30] M. Van den Nest, J. Dehaene, and B. De Moor, Phys. Rev. A **69**, 022316 (2004).
[31] G. Gilbert, M. Hamrick, and Y.S. Weinstein, Phys. Rev. A **73**, 064303 (2006).
[32] C.M. Dawson, H.L. Haselgrove, and M.A. Nielsen, Phys. Rev. Lett. **96**, 020501 (2006).
[33] M. Varnava, D.E. Browne, and T. Rudolph, Phys. Rev. Lett. **97**, 120501 (2006).